



**HAL**  
open science

# Nonlinear dynamics of a laser diode subjected to both optical injection and optical feedback

Lucas Oliverio, Damien Rontani, Marc Sciamanna

► **To cite this version:**

Lucas Oliverio, Damien Rontani, Marc Sciamanna. Nonlinear dynamics of a laser diode subjected to both optical injection and optical feedback. *Optics Express*, 2024, 32 (15), pp.25906-25918. 10.1364/OE.519374 . hal-04834823

**HAL Id: hal-04834823**

**<https://hal.science/hal-04834823v1>**

Submitted on 12 Dec 2024

**HAL** is a multi-disciplinary open access archive for the deposit and dissemination of scientific research documents, whether they are published or not. The documents may come from teaching and research institutions in France or abroad, or from public or private research centers.

L'archive ouverte pluridisciplinaire **HAL**, est destinée au dépôt et à la diffusion de documents scientifiques de niveau recherche, publiés ou non, émanant des établissements d'enseignement et de recherche français ou étrangers, des laboratoires publics ou privés.

# Nonlinear dynamics of a laser diode subjected to both optical injection and optical feedback

LUCAS OLIVERIO,<sup>1,2,\*</sup> DAMIEN RONTANI,<sup>1,2</sup> AND MARC SCIAMANNA<sup>1,2</sup>

<sup>1</sup>Université de Lorraine, CentraleSupélec, LMOPS, 57070 Metz, France

<sup>2</sup>Chaire Photonique, LMOPS, CentraleSupélec, 57070 Metz, France

\*lucas.oliverio@centralesupelec.fr

**Abstract:** We analyse theoretically the nonlinear dynamics of a single-mode laser diode subjected to both optical injection and optical feedback. Detailed mappings of the laser dynamics reveal that, due to optical feedback (OF), the locking boundaries resulting from optical injection (OI) shift towards larger negative detunings and higher injection rates and display a periodic pattern of the injection locking boundaries. We demonstrate how feedback induces a cascade of quasiperiodic bifurcations associated with abrupt dynamic changes, hence altering the route to locking. A close inspection of the laser optical spectra for increasing feedback rate reveals the complex interplay between undamped relaxation oscillations and external cavity frequencies.

## 1. Introduction

Semiconductor lasers play a critical role in modern telecommunications by enabling high-speed data transmission in optical fiber communication systems. An optically injected laser generates a variety of dynamics, including periodic regimes, chaos, and injection locking [1,2]. Furthermore, under appropriate conditions, the optical injection of chaos into a second laser enables the onset of chaos synchronisation and the related chaos-based secure communications [3–6]. Injecting a polarized field or a single mode into a multi-polarization or longitudinal mode laser creates new opportunities for chaos instabilities while also providing further controls for controlling the dynamics of the system [7,8]. Optical injection is also used for random number generation [9,10], microwave generation [11–13] or enhanced modulation bandwidth [14]. Moreover injection of a delayed optical field -also called optical feedback- creates novel and different instabilities [15–21]. When controlled, these instabilities allow for novel applications such as laser stabilisation [22], optical chaos-based cryptography [3,9,23–28] and interferometric applications [29].

In practice, most of today's applications of nonlinear dynamics combine optical injection and optical feedback, *e.g.*, for the enhancement of chaos bandwidth for information security [30–32], or photonic-based artificial intelligence [33–38]. In that context, it has been shown that a fine-tuning of both optical injection and optical feedback is required to achieve optimal performance in task solving [37,38].

Nevertheless, systematic studies of the laser dynamics and the complexity induced in the presence of both optical feedback and injection remain scarce. Experiments have revealed a shift of the injection locking region when increasing the feedback rate [39,40]. However, theoretical confirmation is still lacking. Nizette *et al.* [41] use asymptotic approximations to demonstrate delay-periodic oscillations in the injection locking bifurcation boundaries with increasing feedback rate. There is therefore this asymptotic and theoretical study that predicts an oscillation of the locking boundary when feedback is applied, but does not really address the dynamics of the laser. Experimental studies, on the other hand, suggest a shift in the locking region and even an increase in the complexity of the injection dynamics, but no oscillation of the locking limit. There is a need for a theoretical, systematic, detailed and coherent study of the dynamics of a laser diode under optical injection and optical feedback.

<https://doi.org/10.1364/OE.519374>

Received 31 Jan 2024; revised 13 May 2024; accepted 4 Jun 2024; published 2 Jul 2024

In this paper, we perform in-depth numerical investigations of a semiconductor laser subjected to both optical injection and optical feedback. This study, which begins with very low feedback rates, provides insights into the impact of parasitic feedback in an optical injection system. We clarify earlier claims by studying the effect of increasing optical feedback rate on the injection locking boundaries and the dynamic properties. More specifically, we highlight how optical feedback deeply alters the route to chaos or locking by demonstrating the emergence of what we call a cascade of quasiperiodic bifurcations, going from simple time-periodic dynamics to complex regimes through secondary feedback-induced bifurcations. We contrast the impact of the feedback depending on the time-delay value [42]. Finally, we emphasise feedback's effects on specific dynamics that bifurcate from the injection locking: (i) wave mixing from the saddle-node bifurcation line, (ii) time-periodic dynamics from the Hopf bifurcation line, (iii) injection-induced chaotic regimes next to the Hopf bifurcation line.

## 2. Numerical model

We consider a single mode rate equation extended to account for optical injection and optical feedback as follows [15]:

$$\frac{dE(t)}{dt} = \frac{(1 + i\alpha)}{2} \left[ G [N(t) - N_0] - \frac{1}{\tau_{ph}} \right] E(t) + \kappa_f E(t - \tau) e^{-i\omega\tau} + \kappa_{inj} A e^{-i\Delta\omega t}, \quad (1)$$

$$\frac{dN(t)}{dt} = \frac{1}{\tau_s} [pN_{th} - N(t)] - G [N(t) - N_0] |E|^2 \quad (2)$$

where  $E(t)$  is the slow varying amplitude of the complex electric field;  $N(t)$  is the carrier density;  $\alpha$  is the linewidth enhancement factor.  $\tau_{ph}$  is the photon lifetime.  $\tau_s$  is the carrier lifetime;  $G$  is the gain coefficient;  $N_0$  is the carrier density at transparency;  $\kappa_f$  is the feedback rate;  $\tau$  is the length of the delay line;  $\kappa_{inj}$  is the injection rate;  $p = I/I_{th}$  is the normalised injection current;  $N_{th} = N_0 + \frac{1}{G\tau_{ph}}$  is the carrier density at threshold;  $\Delta\omega$  is the angular frequency detuning ( $\Delta\omega = 2\pi\Delta f = 2\pi(f_d - f_r)$ ) between the drive and the response laser.  $A$  is the steady-state solution of the electric field amplitude of a single-mode semiconductor laser.

The values of the parameters used in the numerical simulations are presented in Table 1. We work with short delays (less than 3 ns) and a low current  $I = 1.015I_{th}$ . This is motivated in

**Table 1. Parameter values used in numerical simulations**

Symbol	Parameter	Value
$\alpha$	Linewidth enhancement factor	5.0
$\tau_{ph}$	Photon lifetime	$2.0 \times 10^{-12}$ s
$\tau_s$	Carrier lifetime	$2.01 \times 10^{-9}$ s
$G$	Gain coefficient	$7.0 \times 10^4$ s <sup>-1</sup>
$N_0$	Carrier density at transparency	$1.680 \times 10^8$
$\kappa_f$	Feedback rate	[0 – 10] GHz
$\kappa_{inj}$	Injection rate	[0 – 60] GHz
$\Delta\omega$	Detuning	[-18; 7] GHz
$\tau$	Feedback delay time	1 ns to 3 ns
$p$	Normalised injection current	1.015
$N_{th}$	Carrier density at threshold	$2.394 \times 10^8$
$A$	Steady-state amplitude	$3.573 \times 10^3$

particularly by neuromorphic applications based on laser diodes subjected to simultaneous optical injection and optical feedback, such as delay reservoir computing [43]. Indeed, the literature shows the best performance near the laser threshold [44]. We apply a second-order Runge-Kutta method to integrate Eqs. (1)–(2). In our simulations, we consider a range of [0 – 20] GHz feedback rate and [0 – 60] GHz injection rate which corresponds in our system to [0 – 17] % of feedback ratio and [0 – 51] % of injection ratio compared to stationary laser power with  $\kappa(\%) = \kappa(\text{GHz}) \tau_L$ , where  $\tau_L = 8.5 \times 10^{-12}$  s is the internal round trip time.

### 3. Mapping of dynamics with both optical injection and optical feedback

In this section, we analyse the impact of the gradual introduction of optical feedback on the mapping of the optical injection dynamics. We sweep two parameters, the injection rate  $\kappa_{inj}$  and the detuning  $\Delta\omega$  at a fixed pumping current of  $1.015 I_{th}$  and a feedback delay-time  $\tau = 3$  ns. The influence of optical feedback is shown in Fig. 1, with a serie of maps for a range of feedback rates, starting from 0 (no feedback) to 0.60 GHz (small feedback rate of 0.51 % compared to stationary laser power). These maps are colour-coded, where each colour corresponds to a number of major peaks in the optical spectrum obtained numerically from the Fourier transform of the complex optical field. The central triangle-shaped region (deep blue colour) delimits the injection locking zone, and lighter blue to yellow represents time-periodic dynamics with different periods. Red regions reveal over 15 peaks in their optical spectrum, showcasing rich and complex spectra, generally associated with chaos.

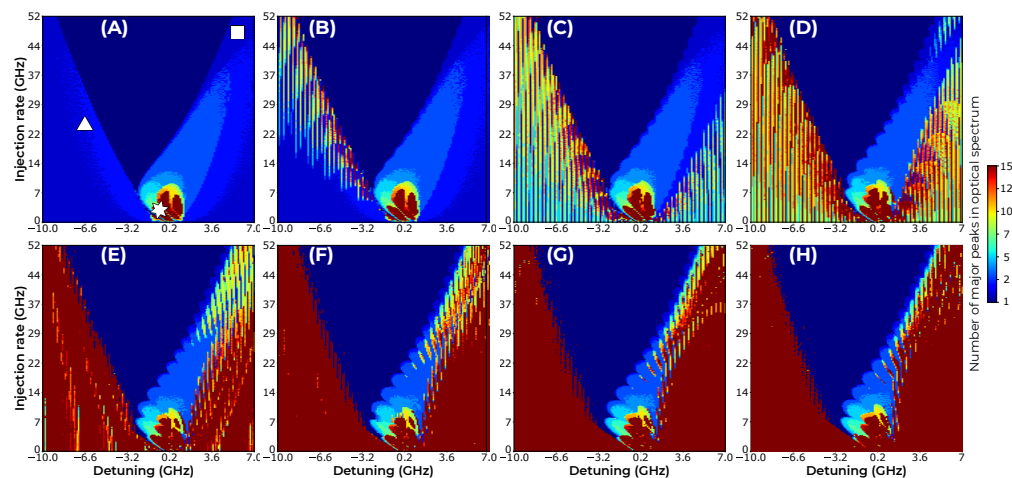


**Fig. 1.** Maps of the dynamics of the injected laser diode in the injection-detuning parameter space. Feedback time delay  $\tau = 3$  ns. Feedback rate  $\kappa_f =$  (A) 0, (B) 0.05, (C) 0.10, (D) 0.20, (E) 0.30, (F) 0.40, (G) 0.50 and (H) 0.60 GHz. The colour codes the number of major peaks in the optical spectrum; dark blue: injection-locking; red: complex dynamics close to chaos or chaotic. On map (A), the triangle, square and star are the three scenarios studied in section 6.

Without feedback, in Fig. 1(A), the system exhibits a well-known dynamic map: a saddle-node (SN) bifurcation line delimits the triangular-shaped locking region for negative detuning values and a Hopf bifurcation line delimits the region for the positive detuning values. Additionally, a chaotic region is observed from the Hopf bifurcation line in weakly positive detunings and low injection rates, consistent with literature [4]. At a very low feedback rate  $\kappa_f = 0.05$  GHz, in Fig. 1(B), the locking area slightly expands and the Hopf bifurcation line exhibits a periodic structuring with low amplitude. For negative detunings, under the SN bifurcation line, spectra

become more complex and the feedback introduces periodically dynamics transitions with a periodicity of  $\Delta\omega \propto 1/\tau$ , hence yielding a periodic structuring of the map of dynamics. As the feedback rate increases in Fig. 1(C) and (D)  $\kappa_f = 0.1$  GHz and 0.2 GHz, spectra exhibit increasing complexity i.e. the colour code tends towards red. The Hopf bifurcation line oscillates with a period  $\Delta\omega = 1/\tau$  in detuning. In panels (E), (F), (G), and (H), with feedback rates of 0.3, 0.4, 0.5, and 0.6 GHz, respectively, the destabilisation and complexification of the spectra continues, following the trend described in the previous map. We also notice that the oscillation is not limited to the Hopf bifurcation line in positive detunings, the nested bifurcations under the Hopf bifurcation line, including the chaotic region, see their boundaries also oscillating with  $\Delta\omega \propto 1/\tau$ . The SN bifurcation line exhibits also a  $1/\tau$ -periodic structuring in detuning, but it differs from that of the Hopf bifurcation. We also observe that dynamics become essentially chaotic outside the injection locking region visible in red. We observe that the transitions to locking through the SN and the Hopf bifurcation lines are notably different: from the SN we have a sharp and abrupt transition towards highly chaotic spectra. In contrast, when crossing the Hopf bifurcation, we observe a smoother transition to locking.

Earlier experiments have measured that the locking region shifts towards negative detunings in the presence of optical feedback [39,40]. Our measures of the vertical and horizontal shift of the zone confirm and detail this behaviour. In 2015, Song *et al.* [40] used a laser diode with both optical injection and optical feedback but based on a fiber Bragg grating (FBG) mirror. Given their feedback delay (about 30 ns), the period of the Hopf bifurcation oscillation is expected to be about  $\Delta\omega \approx 33$  MHz in detuning. We assume that their limited experimental resolution prevented them from seeing the appearance of the cascade of quasi-periodic bifurcations or the Hopf bifurcation line. We assume the same limitation in Liao *et al.* in 2013 [39], where the long delay (about 80 ns) leads to an oscillation with a periodicity of about  $\Delta\omega \approx 12$  MHz.

Similar oscillations of the injection locking (IL) bifurcation boundaries for increasing feedback rates have also been predicted by Nizette *et al.*, but without the IL shift [41]. However, the theory was performed with a simplified normalised model, using asymptotic assumptions (low feedback rate, low injection rate, large delay). Our study, employing a full model without approximations, enables us to obtain an accurate representation for comparison with the approximate prediction derived from an asymptotic study. Even with the same parametric conditions as in the theoretical study, we show that the IL zone shifts as soon as feedback is applied and we do not see the oscillation of the locking limits. The oscillation we show here is only visible at higher injection rates and detuning values than in the asymptotic study.

#### 4. Contrasting long and short cavity regimes

We compare the impact of the feedback delay time on the injection locking boundaries. The period of the relaxation oscillation being  $\tau_{RO} = 2.1$  ns, the previous delay time of 3 ns is considered as a long cavity [45]. We compare here a feedback delay time of  $\tau = 1$  ns with  $\tau = 3$  ns. Figure 2 shows four dynamic maps of the locking area in the  $(\kappa_{inj}; \Delta\omega)$  plane for various parameters. Figure 2(A) is obtained with a feedback rate of 0.9 GHz and a 1 ns delay ( $< \tau_{RO}$ ), corresponding to a short-cavity regime. Similarly to Fig. 1, the feedback transforms the boundaries of the locking area, leading to oscillations in the bifurcation lines. The Hopf bifurcation line periodically oscillates, while the SN bifurcation line shows a more abrupt transition and less regular oscillation. Both oscillations in the bifurcation lines have a period  $\Delta\omega \propto 1/\tau = 1$  GHz in detuning. Figure 2(B) is produced with a low feedback rate (0.9 GHz) and a 3 ns delay. The Hopf bifurcation line is again  $1/\tau$ -periodic at 0.33 GHz. Interestingly, the SN bifurcation line is irregular and non-periodically structured. Figure 2(C) is generated with a strong feedback rate (10 GHz) and a delay time of 1 ns. We observe that the locking region has shifted by nearly 9 GHz towards the negative detunings and also towards higher injection rates. The oscillation of the Hopf bifurcation line still exists at a periodicity of  $1/\tau$ , but its amplitude has

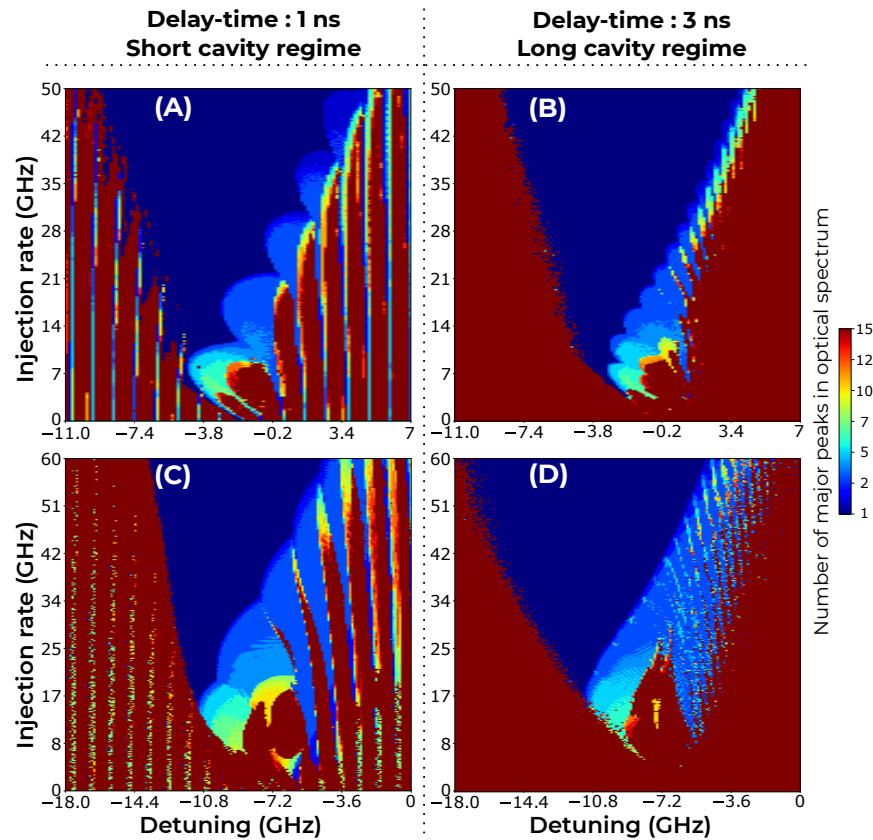


**Fig. 2.** Comparison between short delay and long delay for weak and strong feedback. (A) & (B): weak feedback  $\kappa_f = 0.9$  GHz. (C) & (D): strong feedback  $\kappa_f = 10$  GHz. Horizontal axes are different depending on the feedback rate to take account of the injection locking region shift.

decreased significantly, making it less noticeable. On the other hand, the saddle-node bifurcation line remains non-oscillatory and almost smooth. Figure 2(D) is made with a strong feedback rate (10 GHz) and a delay time of 3 ns. The locking area has shifted due to the optical feedback. The oscillation of the Hopf bifurcation line is still present but with a strongly damped amplitude, becoming almost indiscernible. The saddle-node bifurcation line, in this case, is irregular and lacks periodic structure. Compared to Fig. 2(C), we note that the injection locking region is wider for a similar level of injection. In each of the four cases studied, we focus our attention on the injection locking zone and its behaviour. If we now look at the effects of various delays and feedback rates in the unlocked regimes, we see that periodic P1 regimes (color from dark blue to green) from the Hopf bifurcation persist in all maps, even with a strong feedback rate of 10 GHz. This behaviour was previously observed in Fig. 1 for low to moderate feedback rates. The robustness of periodic regimes from the Hopf bifurcation in an optically injected system even at a moderate feedback rate agrees with experimental observations [40].

According to our findings and in agreement with recent experiments [39,40], increasing feedback rate shifts the injection locking area towards negative detunings and higher injection rates. In Fig. 3 we measure the horizontal (detuning) and vertical (injection rate) shift in the case of both short (1 ns) and long (3 ns) delays with feedback. The value of the horizontal shift is considered relative to that without feedback,  $\Delta\omega_{RelativeShift} = \omega_{OI+OF} - \omega_{OI}$ . The same procedure

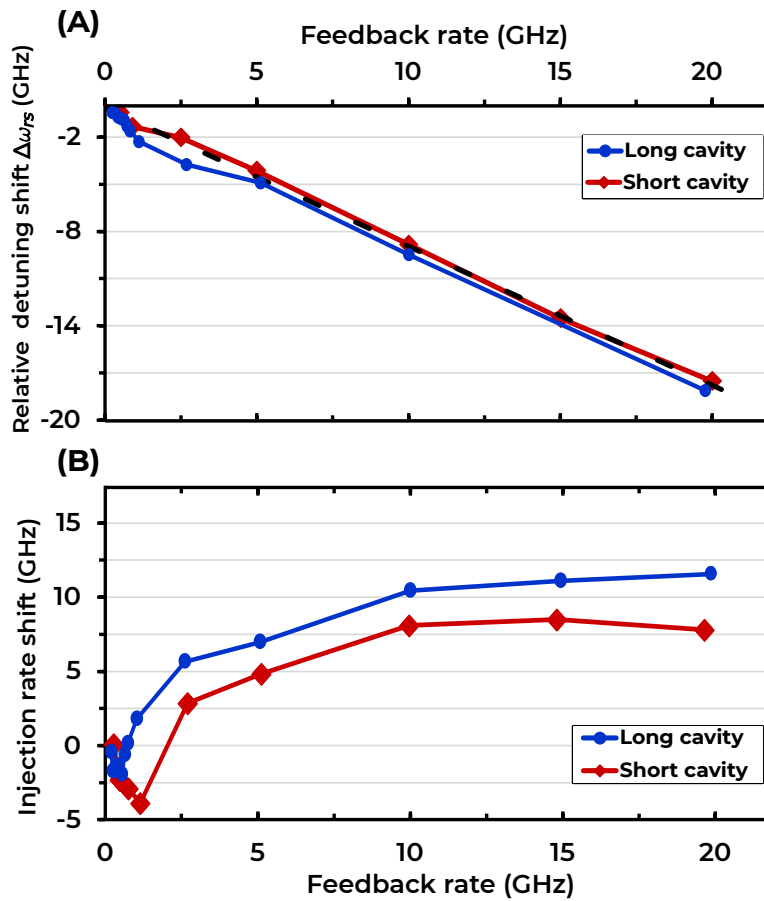


**Fig. 3.** (A) Horizontal and (B) Vertical shift of the injection locking region as a function of feedback rate.

is used for the vertical shift value. In Fig. 3(A), we plot the IL horizontal shift from 0 GHz to 20 GHz of feedback rate. It evolves linearly within the considered feedback rate range: a linear regression gives a slope of  $-0.88$  GHz of detuning per GHz of feedback with  $R^2 > 0.99$  regardless of the feedback delay time. There is a slight difference between 0 and 5 GHz, but this disappears for larger feedback rate values. In Fig. 3(B), we depict the IL vertical shift in injection rate as a function of the feedback rate for both short and long cavities. There is a non-monotonic trend, with a shift toward weaker injection rates for  $\kappa_f < 2$  GHz, which is due mainly to the deformation of the IL region. Then, the locking region shifts towards higher injection rates. We also observe an apparent saturation of the vertical shift, unlike the horizontal shift. The behaviour is similar for the two cavity regimes, thus indicating that a higher injection rate is required to lock the laser when subjected to feedback.

To our knowledge, no experimental study has revealed such oscillations of the locking injection boundaries of a laser subjected to optical injection and feedback. Our analysis shows that to observe these oscillations, the detuning steps must be performed at a resolution close to the inverse of  $\tau$ , and the feedback rate must be low.

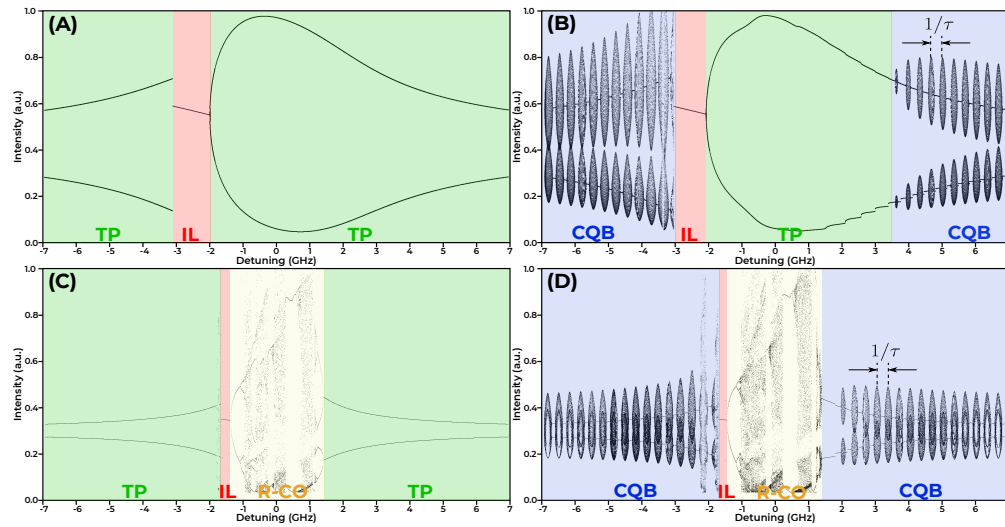


**Fig. 4.** Bifurcation diagram, comparing two injection rates without and with feedback. The colour codes the dynamic regime: IL = Injection Locking. TP = Time-Periodic. R-CO = Route to Chaos & Chaotic Oscillations. CQB = Cascade of Quasiperiodic Bifurcations.  $(\kappa_{inj}, \kappa_f) =$  (A) (12;0) GHz. (B) (12;0.1) GHz. (C) (3.2;0) GHz. (D) (3.2;0.1) GHz.

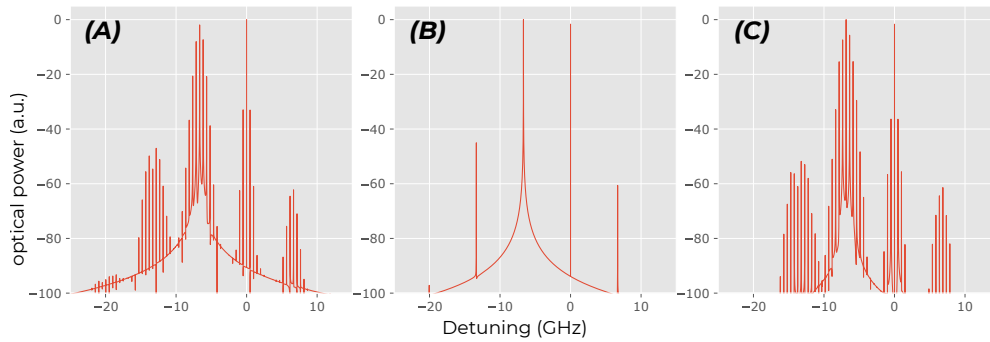


**Fig. 5.** Optical spectra of laser subjected to optical injection and optical feedback in the cascade of quasiperiodic bifurcations.  $\kappa_{inj} = 30$  GHz,  $\kappa_f = 0.1$  GHz,  $\Delta\omega =$  (A)  $-6.5$  GHz, (B)  $-6.85$  GHz, (C)  $-7.15$  GHz.

## 5. Cascade of quasiperiodic bifurcations in the route to locking

In this section, we investigate the periodically repeating changes outside the locking region seen in Fig. 1(B) to (E) with weak feedback rate. Figure 4 depicts the corresponding bifurcation diagram of the maxima and minima of the output intensity of the laser. The control parameter is the detuning  $\Delta\omega \in [-7; 7]$  GHz.

In Fig. 4(A) without feedback, the injection rate is set to 12 GHz. For the  $\Delta\omega$  interval in red, the laser is in the IL regime. For larger  $\Delta\omega$ , the system undergoes a Hopf bifurcation and for smaller and negative detunings, the system undergoes a SN bifurcation. Figure 4(B) corresponds to the same injection rate but with 0.1 GHz of feedback rate. Outside locking through SN bifurcation the laser enters in a cascade of quasiperiodic bifurcations. The periodicity of these repeating bifurcations is  $\Delta\omega \approx 1/\tau = 1/3 = 0.33$  GHz. A similar cascade is observed after the Hopf bifurcation in the positive detunings beyond  $\Delta\omega = 3$  GHz. In Fig. 4(C) without feedback,

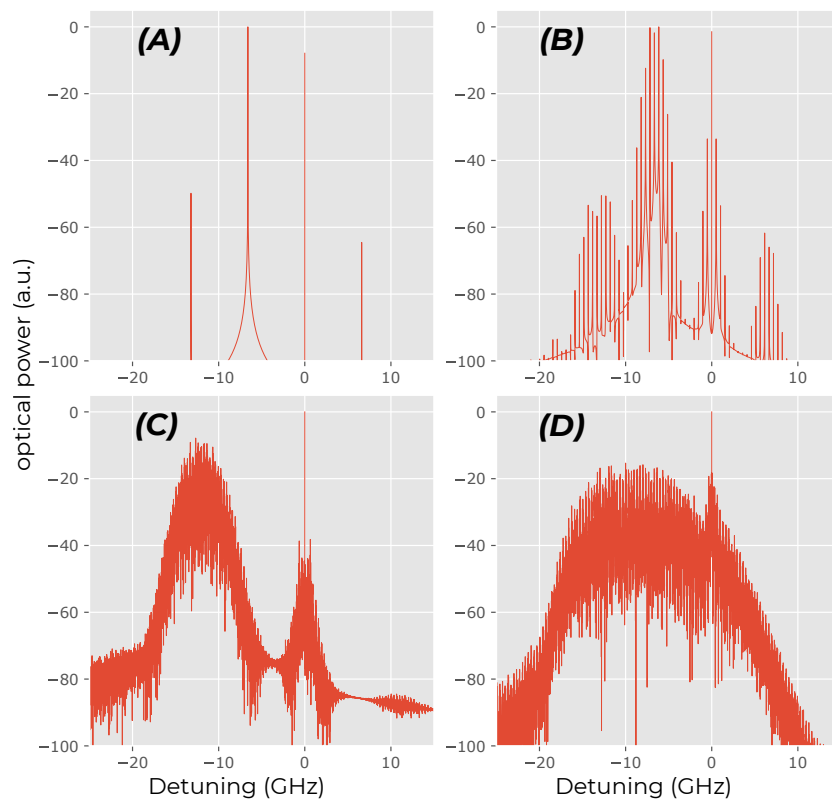
the injection rate is set to 3.2 GHz. We have a quite classical bifurcation diagram with the laser being chaotic in  $\Delta\omega = [-1; 1.2]$  GHz next to injection locking. In Fig. 4(D) for 0.1 GHz of feedback rate, we see that the chaotic regime and the injection locking regime are almost unchanged. However, periodic dynamics occurring in positive and negative detunings undergo periodically repeating quasiperiodic bifurcations.

Figure 5 details the optical spectra recorded when sweeping  $\Delta\omega$  through one of the quasiperiodic bifurcations induced by feedback. In Fig. 5(A), we observe a quasiperiodic wave mixing (QP WM) supplemented with frequencies ( $f_{RO}$ ). In Figure (B), detuning is shifted by 0.35 GHz leading to a periodic wave mixing with a periodicity equal to the detuning. Then, in Figure (C), detuning is again shifted by 0.35 GHz and the optical spectrum is again a QP WM. Thus, we confirm that the system alternates between time-periodic and quasiperiodic dynamics. This phenomenon occurs periodically with detuning, at  $1/\tau$ , or every  $\Delta\omega = 0.33$  GHz.

## 6. Analysis of the impact of feedback on typical injection dynamics

### 6.1. Wave-mixing from the Saddle-Node bifurcation line

In this section, we make a closer inspection of a first dynamical scenario, and how feedback affects the typical dynamics of a laser diode with OI. We start with the WM between the drive



**Fig. 6.** Scenario 1: wave mixing from the saddle-node bifurcation line. Optical spectra of laser subjected to optical injection with  $\kappa_{inj} = 24$  GHz. Feedback rate and detuning  $(\kappa_f; \Delta\omega) =$  (A) (0 GHz; -6.5 GHz), (B) (0.05 GHz; -6.5 GHz), (C) (2.5 GHz; -13 GHz) & (D) (10 GHz; -13 GHz). Detuning is changed to take account of the shift in the locking zone.

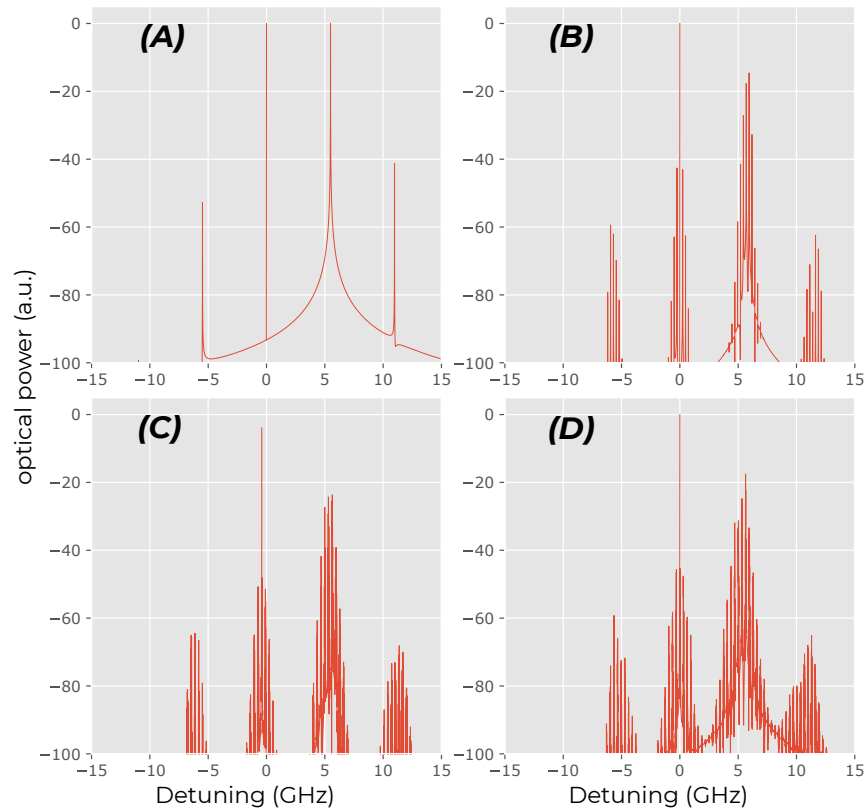


**Fig. 7.** Scenario 2: time-periodic dynamics from the Hopf bifurcation line. Optical spectra of laser subjected to optical injection with  $\kappa_{inj} = 50$  GHz and detuning  $\Delta\omega = 5.5$  GHz. Feedback rate  $\kappa_f =$  (A) 0 GHz, (B) 0.9 GHz, (C) 2.5 GHz & (D) 5 GHz.

and the response laser emerging from the SN bifurcation of the locked steady state. As shown in Fig. 6(A), without feedback, the WM creates P1 dynamics with a periodicity equal to the detuning value. In Fig. 6(B), we use 0.05 GHz feedback rate while keeping all other parameters constant. The overall structure of P1 WM is preserved in the optical spectra (B). Feedback yields undamped relaxation oscillations around each peak. These new frequencies corresponding to relaxation oscillations are spaced by 0.5 GHz. The spectrum in Fig. 6(C) with feedback rate of 2.5 GHz shows degradation in the WM shape, exhibiting spectral broadening, with a disappearance of the WM harmonics. We find  $f_{RO}$  subharmonics. Plus, external cavity frequency (ECF) is seen in the spectrum as a series of periodic peaks. These peaks are precisely spaced at 0.33 GHz, corresponding to  $1/\tau$ . In Fig. 6(D) with a feedback rate of 10 GHz, we can observe that the WM structure has disappeared, and the spectrum is chaotic and wide (bandwidth about 15 GHz). Peaks related to ECF and thus to the delay are visible. The  $f_{RO}$  signature has completely vanished, indicating that the feedback dynamics have taken precedence over the injection dynamics.

In conclusion, we show that feedback yields undamped relaxation oscillations resulting eventually in significant spectral broadening. Feedback dynamics become dominant over injection dynamics. We see that the threshold at which feedback becomes dominant is very low (less than one GHz of feedback rate), as we can see on the dynamic maps. The external cavity frequencies exacerbated the chaotic dynamic, finally supplanting the original dynamic (P1 in chaos). Therefore next to the Saddle-Node bifurcation line, feedback induces secondary bifurcations on time-periodic dynamics that lead to chaos.

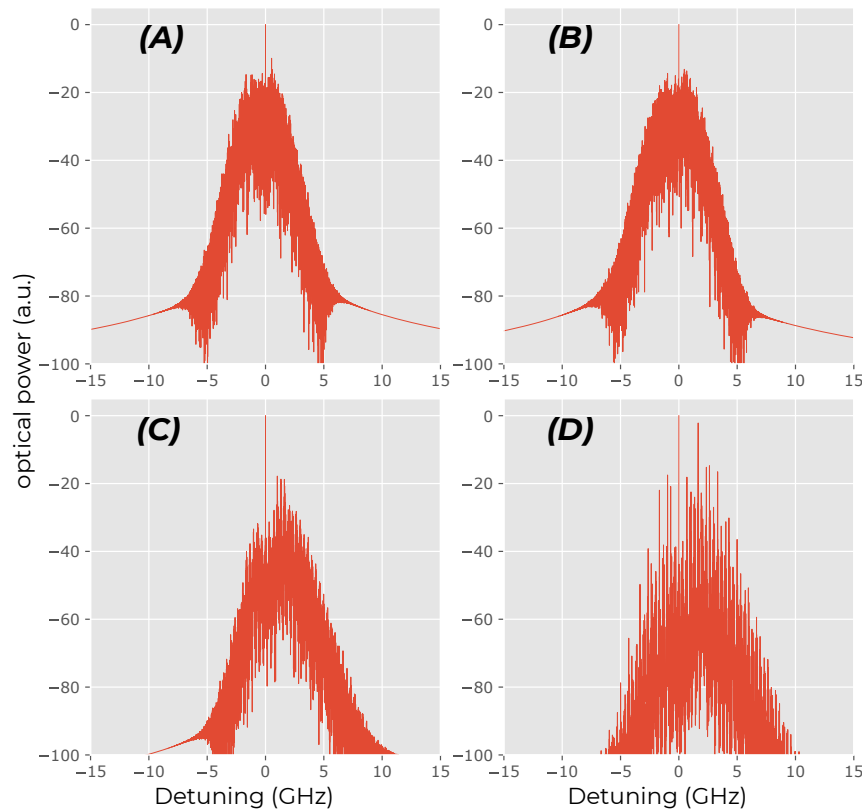


**Fig. 8.** Scenario 3: chaos under the Hopf bifurcation line. Optical spectra of laser subjected to optical injection and optical feedback. Injection rate, feedback rate and detuning  $(\kappa_{inj}; \kappa_f; \Delta\omega) =$  (A) (2.5 GHz; 0 GHz; -0.5 GHz), (B) (2.5 GHz; 0.4 GHz; -0.5 GHz), (C) (2.5 GHz; 2.5 GHz; -1 GHz) & (D) (10 GHz; 5 GHz; -3.5 GHz).

## 6.2. Time-periodic dynamics from the Hopf bifurcation line

In this section, we study the feedback influence on the spectral components of time-periodic dynamics near the Hopf bifurcation line. In Fig. 7(A) without feedback, we see P1-dynamics originally triggered by the undamping of relaxation oscillations at the Hopf bifurcation line. Figure 7(B) with a feedback rate of 0.9 GHz shows that each peak is surrounded by new frequencies close to  $f_{RO}/2$  and  $1/\tau$ , implying a complex interaction between these two time scales. We understand that there is a competition between ECFs and  $f_{RO}$  as expected from the literature [3]. With  $\kappa_f = 3$  GHz in Fig. 7(C), we observe new frequency components next to the previous P1 peaks. The overall P1 structure is still visible. The presence of  $f_{RO}$ , which had appeared in the previous figure, has vanished; with no peak around  $f_{RO} = 0.5$  GHz. In Fig. 7(D), with  $\kappa_f = 5$  GHz, we observe similar characteristics to those seen for  $\kappa_f = 3$  GHz. In other words, the optical spectrum still exhibits a global P1 structure, with multiple additional frequencies, leading to quasiperiodicity. Unlike scenario 1, the spectral broadening is here limited. The P1 peaks are surrounded by peaks with a frequency spacing of about 8 MHz, which corresponds to subharmonics of the external cavity fundamental frequency at  $F_{ECF}/41$ .

In conclusion, we investigated how feedback affects spectral properties of dynamics emerging from the Hopf bifurcation. We find that time periodic dynamics is supplemented with new frequencies. Increasing feedback rate adds relaxation oscillation and external cavity frequencies

and preserves quasiperiodicity (QP), the dynamic regime does not become chaotic like near the SN bifurcation line in scenario 1. This shows how in dynamic maps, even with feedback, P1 and QP regimes persist next to the Hopf bifurcation line even at a high feedback rate. The structure of the final optical spectrum differs significantly from the scenario with the SN bifurcation line.

### 6.3. Chaotic states near the Hopf bifurcation line

Here we investigate the effects of feedback on chaotic regimes induced by OI. We chose to work within the "chaotic bubble" located below the Hopf bifurcation line (see star-shaped point in Fig. 1(A)).

In Fig. 8(A), we choose  $\Delta\omega = -0.5$  GHz and  $\kappa_{inj} = 2.5$  GHz without feedback. The optical spectrum (A) shows a chaotic regime with a bandwidth of  $\sim 10$  GHz revealed by the presence of a continuum of frequencies. Harmonics are recorded at 1 GHz and are approximately uniformly spaced, implying chaos caused by wave mixing involving  $f_{RO}$ . Panel (B) is similar to (A) with a 0.4 GHz feedback rate. Panel (C) is obtained with a higher feedback rate of  $\kappa_f = 2.5$  GHz and  $\Delta\omega = -1$  GHz. To "follow" this relatively narrow chaotic zone, we need to change our injection and detuning parameters. The optical spectrum has evolved as a result of feedback. The width has not changed, but it has regular peaks that are reminiscent of the external cavity spectral signatures. Finally, in panel (D), we continue to focus on this specific chaotic bubble with  $\kappa_f = 5$  GHz,  $\kappa_{inj} = 10$  GHz and  $\Delta\omega = -3.5$  GHz. The optical spectrum is slightly wider and has significant regularly spaced peaks corresponding to ECFs.

## 7. Conclusion

In summary, we have analysed the effect of optical feedback on a laser subjected to optical injection, through a systematic analysis of dynamic mapping, bifurcation diagrams and optical spectra. We unveiled how the locking boundaries are modified with increasing feedback rates. The boundary of the injection locking region oscillates with a periodicity linked to the feedback delay time. We also showed that feedback has a profound impact on an optically injected laser's dynamics, producing cascades of quasiperiodic bifurcations. In the  $(\kappa_{inj}; \Delta\omega)$  plane, we identify four significant phenomena: (i) the emergence of a cascade of quasiperiodic bifurcations, (ii) the oscillation of the injection locking boundary, (iii) dynamics that become mainly chaotic outside the locking region, (iv) a shifting of the injection locking zone towards negative detunings and higher injection rates. We started at extremely low feedback rates (0.05 GHz), allowing us to see these phenomena at their earliest stages and their impact at high feedback rates (10 GHz).

We also investigate the impact of feedback on three conventional optical injection dynamics. Feedback yields undamped relaxation oscillations, resulting in significant spectral broadening. When increasing feedback rate, ECFs appear and become dominant, eventually supplanting the original dynamic regime (*e.g.* WM transformed into chaos). On chaotic regimes, we observe that feedback causes chaos broadening and frequency content modification, including the spectral signatures of the external cavity. The transitions to locking through the SN bifurcation line and the Hopf bifurcation line are quite different, abrupt for the SN and smooth for the Hopf. This allows the maintenance of quite robust P1 regimes next to the Hopf bifurcation line. We also discussed the effect of delay on these feedback-related dynamics varying the delay and noted no qualitative difference between a long and short delay apart from increasing or decreasing the prominence of the phenomena described above. Our comprehensive analysis therefore complements earlier theoretical approximations and brings new light to recent experimental observations.

We explored a theoretical framework that offers several intriguing predictions, which we aim to experimentally verify. Two notable phenomena have caught our attention, the cascade of quasiperiodic bifurcations and the oscillations in the Hopf bifurcation boundary. Still, the experimental observation requires a short feedback delay and a moderate feedback rate, presenting certain experimental challenges. Our investigation also delves into the domain of optical injection

applications, particularly in the context of microwave frequency generation. We provide insights into how these systems would behave in the presence of low-level parasitic feedback rate, with a specific focus on their robustness near the Hopf bifurcation line.

**Funding.** Ministère de l'Enseignement supérieur, de la Recherche et de l'Innovation; European Regional Development Fund; Fondation CentraleSupélec; Conseil régional du Grand Est.

**Disclosures.** The authors declare no conflicts of interest.

**Data availability.** Data underlying the results presented in this paper are not publicly available at this time but may be obtained from the authors upon reasonable request.

## References

1. T. B. Simpson, J. M. Liu, K. F. Huang, *et al.*, "Nonlinear dynamics induced by external optical injection in semiconductor lasers," *Quantum Semiclass. Opt.* **9**(5), 765–784 (1997).
2. S. Wiczorek, B. Krauskopf, T. Simpson, *et al.*, "The dynamical complexity of optically injected semiconductor lasers," *Phys. Rep.* **416**(1-2), 1–128 (2005).
3. M. Sciamanna and K. A. Shore, "Physics and applications of laser diode chaos," *Nat. Photonics* **9**(3), 151–162 (2015).
4. T. B. Simpson, J. M. Liu, A. Gavrielides, *et al.*, "Period-doubling route to chaos in a semiconductor laser subject to optical injection," *Appl. Phys. Lett.* **64**(26), 3539–3541 (1994).
5. X.-Q. Qi and J.-M. Liu, "Photonic Microwave Applications of the Dynamics of Semiconductor Lasers," *IEEE J. Sel. Top. Quantum Electron.* **17**(5), 1198–1211 (2011).
6. J. Mercadier, Y. Doumbia, S. Bittner, *et al.*, "Optical chaos synchronization in a cascaded injection experiment," *Opt. Lett.* **49**(10), 2613–2616 (2024).
7. I. Gatara, M. Sciamanna, J. Buesa, *et al.*, "Nonlinear dynamics accompanying polarization switching in vertical-cavity surface-emitting lasers with orthogonal optical injection," *Appl. Phys. Lett.* **88**(10), 101106 (2006).
8. D. S. Wu, R. Slavik, G. Marra, *et al.*, "Direct Selection and Amplification of Individual Narrowly Spaced Optical Comb Modes Via Injection Locking: Design and Characterization," *J. Lightwave Technol.* **31**(14), 2287–2295 (2013).
9. R. Vicente, J. Dauden, P. Colet, *et al.*, "Analysis and characterization of the hyperchaos generated by a semiconductor laser subject to a delayed feedback loop," *IEEE J. Quantum Electron.* **41**(4), 541–548 (2005).
10. X.-Z. Li and S.-C. Chan, "Random bit generation using an optically injected semiconductor laser in chaos with oversampling," *Opt. Lett.* **37**(11), 2163 (2012).
11. S.-C. Chan, S.-K. Hwang, and J.-M. Liu, "Period-one oscillation for photonic microwave transmission using an optically injected semiconductor laser," *Opt. Express* **15**(22), 14921 (2007).
12. S.-C. Chan, "Analysis of an Optically Injected Semiconductor Laser for Microwave Generation," *IEEE J. Quantum Electron.* **46**(3), 421–428 (2010).
13. T. B. Simpson, J.-M. Liu, M. AlMulla, *et al.*, "Linewidth Sharpening via Polarization-Rotated Feedback in Optically Injected Semiconductor Laser Oscillators," *IEEE J. Sel. Top. Quantum Electron.* **19**(4), 1500807 (2013).
14. T. Simpson and J. Liu, "Enhanced modulation bandwidth in injection-locked semiconductor lasers," *IEEE Photonics Technol. Lett.* **9**(10), 1322–1324 (1997).
15. R. Lang and K. Kobayashi, "External optical feedback effects on semiconductor injection laser properties," *IEEE J. Quantum Electron.* **16**(3), 347–355 (1980).
16. B. Daino, P. Spano, M. Tamburrini, *et al.*, "Phase noise and spectral line shape in semiconductor lasers," *IEEE J. Quantum Electron.* **19**(3), 266–270 (1983).
17. G. Agrawal, "Line narrowing in a single-mode injection laser due to external optical feedback," *IEEE J. Quantum Electron.* **20**(5), 468–471 (1984).
18. L. Goldberg, H. Taylor, A. Dandridge, *et al.*, "Spectral Characteristics of Semiconductor Lasers with Optical Feedback," *IEEE Trans. Microwave Theory Tech.* **30**(4), 401–410 (1982).
19. G. H. M. van Tartwijk and D. Lenstra, "Semiconductor lasers with optical injection and feedback," *Quantum Semiclass. Opt.* **7**(2), 87–143 (1995).
20. K. Petermann, *Laser Diode Modulation and Noise* (Springer Science & Business Media, 1991).
21. K. Petermann, "External optical feedback phenomena in semiconductor lasers," *IEEE J. Sel. Top. Quantum Electron.* **1**(2), 480–489 (1995).
22. R. Tkach and A. Chraplyvy, "Regimes of feedback effects in 1.5- $\mu\text{m}$  distributed feedback lasers," *J. Lightwave Technol.* **4**(11), 1655–1661 (1986).
23. J. Ohtsubo, "Feedback Induced Instability and Chaos in Semiconductor Lasers and Their Applications," *Opt. Rev.* **6**(1), 1–15 (1999).
24. J. Ohtsubo, "Chaos synchronization and chaotic signal masking in semiconductor lasers with optical feedback," *IEEE J. Quantum Electron.* **38**(9), 1141–1154 (2002).
25. H. Fujino and J. Ohtsubo, "Experimental synchronization of chaotic oscillations in external-cavity semiconductor lasers," *Opt. Lett.* **25**(9), 625 (2000).
26. D. Rontani, A. Locquet, M. Sciamanna, *et al.*, "Time-Delay Identification in a Chaotic Semiconductor Laser With Optical Feedback: A Dynamical Point of View," *IEEE J. Quantum Electron.* **45**(7), 879–1891 (2009).

27. S. Sivaprakasam and K. A. Shore, "Demonstration of optical synchronization of chaotic external-cavity laser diodes," *Opt. Lett.* **24**(7), 466 (1999).
28. C. Mirasso, P. Colet, and P. Garcia-Fernandez, "Synchronization of chaotic semiconductor lasers: application to encoded communications," *IEEE Photonics Technol. Lett.* **8**(2), 299–301 (1996).
29. S. Donati, G. Giuliani, and S. Merlo, "Laser diode feedback interferometer for measurement of displacements without ambiguity," *IEEE J. Quantum Electron.* **31**(1), 113–119 (1995).
30. A.-B. Wang, Y.-C. Wang, and J.-F. Wang, "Route to broadband chaos in a chaotic laser diode subject to optical injection," *Opt. Lett.* **34**(8), 1144 (2009).
31. A. Wang, Y. Wang, and H. He, "Enhancing the Bandwidth of the Optical Chaotic Signal Generated by a Semiconductor Laser With Optical Feedback," *IEEE Photonics Technol. Lett.* **20**(19), 1633–1635 (2008).
32. D. Rontani, E. Mercier, D. Wolfersberger, *et al.*, "Enhanced complexity of optical chaos in a laser diode with phase-conjugate feedback," *Opt. Lett.* **41**(20), 4637 (2016).
33. F. Dupont, B. Schneider, A. Smerieri, *et al.*, "All-optical reservoir computing," *Opt. Express* **20**(20), 22783 (2012).
34. F. D.-L. Coarer, M. Sciamanna, A. Katumba, *et al.*, "All-Optical Reservoir Computing on a Photonic Chip Using Silicon-Based Ring Resonators," *IEEE J. Sel. Top. Quantum Electron.* **24**(6), 1–8 (2018).
35. K. Kanno, A. A. Haya, and A. Uchida, "Reservoir computing based on an external-cavity semiconductor laser with optical feedback modulation," *Opt. Express* **30**(19), 34218 (2022).
36. I. Bauwens, K. Harkhoe, P. Bienstman, *et al.*, "Influence of the input signal's phase modulation on the performance of optical delay-based reservoir computing using semiconductor lasers," *Opt. Express* **30**(8), 13434 (2022).
37. J. Vatin, D. Rontani, and M. Sciamanna, "Enhanced performance of a reservoir computer using polarization dynamics in VCSELs," *Opt. Lett.* **43**(18), 4497–4500 (2018).
38. L. Oliverio, D. Rontani, and M. Sciamanna, "High-resolution dynamic consistency analysis of photonic time-delay reservoir computer," *Opt. Lett.* **48**(10), 2716 (2023).
39. Y.-H. Liao and F.-Y. Lin, "Dynamical characteristics and their applications of semiconductor lasers subject to both optical injection and optical feedback," *Opt. Express* **21**(20), 23568 (2013).
40. J. Song, Z.-Q. Zhong, L.-X. Wei, *et al.*, "Experimental investigations on nonlinear dynamics of a semiconductor laser subject to optical injection and fiber Bragg grating feedback," *Opt. Commun.* **354**, 213–217 (2015).
41. M. Nizette and T. Erneux, "Stability of injection-locked CW-emitting external-cavity semiconductor lasers," *IEEE J. Sel. Top. Quantum Electron.* **10**(5), 961–967 (2004).
42. M. Sciamanna, P. Mégret, and M. Blondel, "Hopf bifurcation cascade in small-alpha laser diodes subject to optical feedback," *Phys. Rev. E* **69**(4), 046209 (2004).
43. L. Appeltant, M. Soriano, G. Van der Sande, *et al.*, "Information processing using a single dynamical node as complex system," *Nat. Commun.* **2**(1), 468 (2011).
44. K. Hicke, M. A. Escalona-Morán, D. Brunner, *et al.*, "Information Processing Using Transient Dynamics of Semiconductor Lasers Subject to Delayed Feedback," *IEEE J. Sel. Top. Quantum Electron.* **19**(4), 1501610 (2013).
45. M. Sciamanna, T. Erneux, F. Rogister, *et al.*, "Bifurcation bridges between external-cavity modes lead to polarization self-modulation in vertical-cavity surface-emitting lasers," *Phys. Rev. A* **65**(4), 041801 (2002).